A practical diagram to determine the residual longitudinal strength of grounded ship in Northern Sea Route

Do Kyun Kim[a,b], Han Byul Kim[c], Dong Hee Park[d], Mohd Hairil[e], Jeom Kee Paik[f,g,h]

[a]Marine, Offshore and Subsea Technology (MOST) Group, School of Engineering, Newcastle University, Newcastle upon Tyne, UK

[b]Graduate Institute of Ferrous Technology (GIFT), POSTECH, Pohang, South Korea

[c]Hyundai Maritime Research Institute, Hyundai Heavy Industries Co., Ltd., Ulsan, South Korea

[d]Samsung Heavy Industries Co., Ltd., Geoje-si, South Korea

[e]School of Ocean Engineering, Universiti Malaysia Terengganu, Kuala Terengganu, Malaysia
[f]The International Centre for Advanced Safety Studies (The Lloyd's Register Foundation Research Centre of Excellence), Pusan National University, Busan, South Korea
[g]Department of Naval Architecture and Ocean Engineering, Pusan National University, Busan, South Korea
[h]Department of Mechanical Engineering, University College London, London, UK

CONTACT Jeom Kee Paik jeompaik@pusan.ac.kr The International Centre for Advanced Safety Studies (The Lloyd's Register Foundation Research Centre of Excellence), Pusan National University, Busan 46241, South Korea; Department of Naval Architecture and Ocean Engineering, Pusan National University, Busan 46241, South Korea; Department of Mechanical Engineering, University College London, London WC1E 7JE, UK

History : received : 2018-08-31 accepted : 2019-08-12

ABSTRACT

In this study, a useful solution is proposed for assessing the safety of the ship's hull damaged by grounding in Northern Sea Route (NSR) or Arctic sea. In particular, the residual ultimate longitudinal strength of grounding damaged ship can be predicted by the grounding damage index (GDI) concept. Due to the global warming effects, the Arctic glaciers have been gradually melting, and it may bring us the new North Pole routes. However, there are uncertainties on many causes that can cause grounding accident of the commercial vessels. In this regard, residual ultimate longitudinal strength of grounding damaged commercial ship in Arctic sea is investigated. Five (5) temperatures: room temperature (RT), −20°C, −40°C, −60°C and −80°C were adopted to consider the cold temperature effect in NSR. The Panamax class oil tanker was selected for the investigation of residual ultimate longitudinal strength of grounding damaged ship. Fifty (50) reliable damage scenarios were adopted for the evaluation of structural health by utilising Residual strength versus GDI (R-D) diagram method. From this study, a modified R-D diagram is proposed which can consider grounding damage with cold temperature effect. The obtained outcome will be useful for assessing the safety of the grounded ships in Arctic sea region by measuring the grounding damage amount and surrounding air temperature **[Q1]**.

KEYWORDS

Arctic condition; cold temperature; ultimate longitudinal strength; Panamax class oil tanker; grounding damage

FUNDING

This work was supported by Pohang University of Science and Technology, Technology Innovation Program (grant number: 10053121 and 10051279) and **[Q2]**Ministry of Trade, Industry & Energy**[Q3]** (MI, Korea).

1. Introduction

Northern Sea Route (NSR) may be considered as one of the challenging options to optimise the efficiency of the maritime transportations by saving the operating cost and time. Carbon dioxide has been accelerating the effect of global warming. Hence, many research studies have been conducted on the development of carbon capture and storage technology since early twenty-first century to reduce and minimise the carbon dioxide in the air (IPCC 2005). In addition, it is well recognised that the global warming causes the reducing land–ice cover in the Arctic region. Large efforts have been made for the environment-free development or green growth (IMO 2010). This trend is affecting various fields such as ship yard, civil construction and many others. Moreover, climate change may bring various negative impacts such as acidification of the ocean and potential contribution to severe winters in mid-latitude regions (ScienceDaily 2018). Especially this year (2018), there have been many problems caused by the heat wave around the world.

On the other hand, this global warming may bring the opportunity to open an alternative route, NSR. This is due to the effect of climate change, which has accelerated the sea ice retreat in the Arctic region (Windén et al. 2014). In the case of a new opportunity, global warming has especially given the additional options for commercial maritime navigation through NSR in summer (Kim et al. 2012a; Park 2015). NSR may significantly reduce the navigational distance between Asia and Europe by about 40%, also the period of shipping round 35%, as shown in Figure 1. The details may be referred to Table A1 which shows the distances and potential days saved for Asian transport from Kirkenes (Nowary) and Murmansk (Russia) and Table A2. From the given information, it is found that the climate in NSR is not similar to that in Southern Sea Route (SSR). The season in NSR can be characterised by a long and cold winter season as well as a short and cool summer season. The detailed temperatures, including normal and extreme condition and ice thickness, are also summarised in Table A2 (Emmerson and Lahn 2012).

Figure 1. Comparison between shipping routes. (This figure is available in colour online.)

From a safety design perspective, reducing the uncertainties is one of the key elements for reducing the risk, also for the robust design of the ships and offshore structures (Paik 2018). For ensuring the safe voyage of vessels, the route selection, by identifying the potential risks, should be confirmed in the early design stage to minimise the uncertainties (Mazaheri et al. 2016). In spite of these efforts from various parties, a number of accidents are still occurring and have been steadily reported by IMO (2018), as shown in Table 1 (SNAK 2015). Such parties include classification societies, heavy industries, and research institutions.

Table 1. History of major accidents for various vessels in normal sea route (IMO 2018).

	1995–2000			2001–2005			2006–2010			2011–2014			
Type	A	B	C	A	B	C	A	B	C	A	B	C	Total
Collision	0	3	5	2	15	18	4	11	24	6	11	25	124 (27.2%)
Grounding	0	2	1	1	11	4	13	20	9	1	12	6	80 (17.5%)
Contact	0	0	0	0	6	0	3	21	0	2	9	1	42 (9.2%)
Fire/Explosion	0	2	2	1	11	5	10	16	3	6	14	3	73 (16.0%)
Hull failure	0	0	0	1	0	0	5	2	1	3	1	0	13 (2.9%)
Capsize/Listing	0	0	0	0	1	0	7	6	1	0	21	0	36 (7.9%)
Flooding/Foundering	0	0	0	0	0	0	0	0	0	0	2	1	3 (0.7%)
Occupational accident	0	0	0	1	0	7	10	0	24	6	4	18	70 (15.4%)
Others	0	0	0	2	0	0	6	1	1	5	0	0	15 (3.3%)
Total	0	7	8	8	44	34	58	77	63	29	74	54	456

Note: A = Ro-Ro ship, B = Passenger ship, and C = Commercial ship.

Collision, grounding, fire and explosion events are covering over the 60% in total, as illustrated in Table 1. With regard to grounding accidents, one of the cruise ships named 'CONCORDIA' was damaged by grounding in front of Italy Sea in 2012, as shown in Figure 2(a) (Pedersen 2015). Moreover, a bulk carrier named 'PACIFIC CARRIER' was damaged by a collision in front of Sacheon city in South Korea. It was then grounded, and the hull structure was totally broken into two parts due to the 15th Typhoon in 2012 named 'BOLAVEN', as shown in Figure 2(b) (ChosunBiz 2012).

Figure 2. Typical example of grounding damaged vessels. (a) Costa Concordia (a cruise ship), which was grounded in front of Italy Sea (Pedersen 2015). (b) Pacific Carrier (a bulk carrier), which was grounded in South Korea Sea (ChosunBiz 2012) (Left = first grounded condition, Right = break into two parts by a typhoon). (This figure is available in colour online.)

In this regard, a number of studies have been conducted to reduce and mitigate the risk of the damage by grounding. Recently, International Ship and Offshore Structures Congress (ISSC 2018) highlighted the importance of the marginal strength of a vessel which is essential to avoid catastrophes by understanding the damage impact. They mentioned that the residual strength should be updated to preserve the crew's life long enough for the safe evacuation. This included rescue planning, even if they fail to prevent the loss of the vessel. In the last few decades, various types of analytical approaches, for assessing the residual ultimate strength of intact and damaged hull girders, have been investigated.

With regard to ultimate limit state (ULS), there are several types of useful methods in calculating the ultimate strength of the ship's hull girder. Progressive hull girder collapse analysis, such as nonlinear finite element method, (NLFEM) based on finite elements is such an example. Besides that, there is the intelligent supersize finite element method (ISFEM) by ALPS/HULL (2014) based on the plate-stiffener separation model, and the idealised structural unit method (ISUM) by Ueda and Rashed (1974, 1984) or called Smith method (Smith 1977) based on the plate-stiffener combination model. Classification societies, such as International Association of Classification Societies (IACS), adopt ISUM or Smith method. Details on the strength and the difference of each method may be referred to as ISSC (2012) and Kim et al. (2013b).

The accuracy of the modified Paik–Mansour method was verified by considering six (6) types of representative hull sections. There were ANSYS NLFEM method (ANSYS 2012), ALPS/HULL ISFEM method (ALPS/HULL 2014), and Common Structural Rules methods proposed by IACS (2006a, 2006b) based on ISUM or Smith method. In the case of damaged hulls by grounding and collision, the extensive studies on residual strength of damaged hull girders have been conducted by using the above-mentioned methods. Smith and Dow (1981) adopted ISUM or Smith method to determine the residual strength of the damaged hull girders by considering the indentation damage. Meanwhile, Paik and Thayamballi (1998) proposed total loss scenarios of a bulk carrier, as shown in Figure A1.

Accidents may happen in NSR once the use of this route is more accelerated due to the effect of global warming. However, there are insufficient research outcomes on the vessels that traversed NSR considering the possible accidents such as collision and grounding. As highlighted, the possibility of NSR (or Arctic region) usage is gradually increased due to the global warming effects in terms of loss of ice and water expands in volume. Therefore, the growth of vessels sailing through the NSR has increased the risk of grounding or collision accidents. In this regard, guidelines or rules may be required to assess the damaged structure in the Arctic region. In addition, an investigation of the safe route, including submarine topology and its environmental data, should be performed urgently.

Concerning this, the safety assessment of grounding damaged ships in NSR is investigated in this study by considering the cold temperature effect at NSR. Previously, the R-D diagram method was proposed to assess the structural safety which suffered accidental or in-service damages and the concept was verified by applying grounding damaged ships (Paik et al. 2012). Basically, the R-D diagram shows the relationship between residual strength performance of the damaged structure and the damage index. In order to establish this diagram, they have defined damage index which has a function of grounding damage characteristics such as location and extent of the damage. The residual ultimate hull girder strength of ship with the corresponding grounding damage scenario can be then calculated. Once the R-D diagram is established, it can be utilised for the first-cut safety assessment of ship right after grounding damage suffered.

Later, the applicability of the R-D diagram was studied by Kim et al. (2014a) by considering the effect of ageing issue and grounding damage of oil tankers. But, the effect of cold temperature on the ultimate hull girder strength of grounded ship needs to be further investigated. Therefore, this study investigates the effect of cold temperature on the grounded ship in Arctic region by providing an advanced R-D diagram.

The insights developed in the present study will be useful to estimate the first-cut structural safety of commercial vessel, which is designed for voyage in SSR, in Arctic conditions.

2. Consideration of potential risk: grounding damage in cold region and its analysis technique

Prior to perform a residual strength analysis for assessing the structural safety of the ship under Arctic condition, the damage types and amounts were defined. In this study, a grounding damage by considering the cold temperature condition was mainly investigated.

2.1. Considerable temperature range of Arctic region for numerical simulation

In general, it is reported that the coldest temperature in Arctic region is approximately −68°C. For the consideration of the effect of cold temperature, temperature ranges from room temperature (RT) to −80°C were targeted. There were five (5) typical temperatures selected for the investigation, which were RT, −20°C, −40°C, −60°C and −80°C. The details on applied material properties and considered Arctic condition to be used for residual ultimate strength analysis are documented in this section.

2.1.1. Application of Arctic condition for target structure

Figure 3 shows the assumed operation condition in Arctic sea by Park et al. (2014, 2015b), who had considered air and seawater temperatures in Arctic sea region. In Arctic sea, the temperature of the contacted structural member under the water surface was set as 0°C (zero Celsius). Meanwhile, above the water surface was affected by air temperature, as represented in Figure 3.

Figure 3. Schematic view of the temperature distribution of Arctic sea-going vessel (e.g. oil tanker). (This figure is available in colour online.)

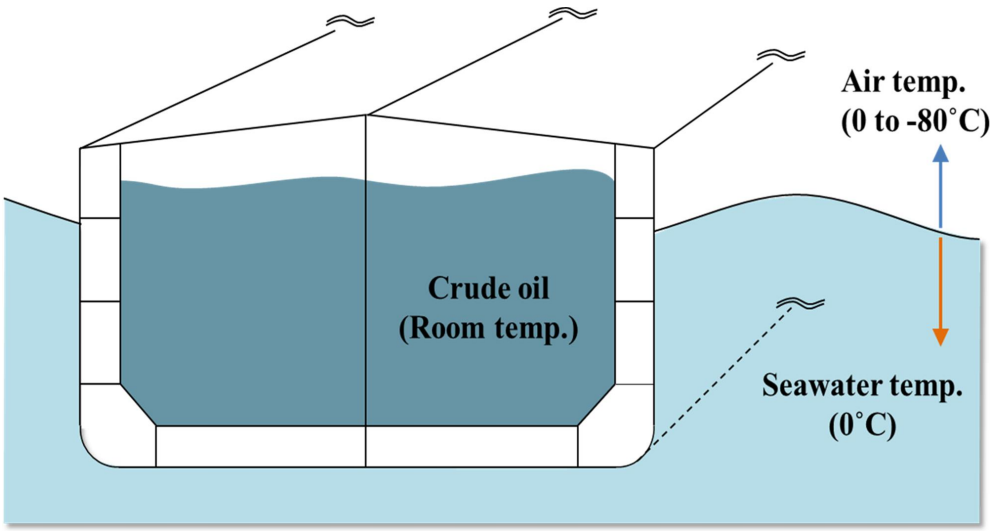

Based on the explanation in Figure 3, the following material properties were applied in this study.

1. Seawater temperature (0°C) was assumed to be applied in structural members under waterline such as the outer side shell and the outer bottom (OB) shell.
2. RT was assumed to be applied in the inner side shell structural members due to oil heating, which was generally

applied to protect the oil coagulation.

3. Cold temperatures (or air temperature in Arctic region = RT to −80°C) were assumed to be applied in structural members above the waterline such as deck and upper outer side shell.

All the above assumptions were made by Park et al. (2014, 2015b) who presented that unfrozen seawater condition should be considered during the voyage in NSR. In addition, seawater temperature (0°C) can be applied to the outer hull structures below the sea level, and the temperatures of the inner side shell can be determined by the cargo type.

2.1.2. Material properties

Bilinear type stress–strain curves obtained by material coupon test under RT, −20°C, −40°C, −60°C and −80°C were adopted for numerical simulation. These temperatures were tested to consider the cold temperature effects for the super aqueous (above the water surface or waterline) structural element in a finite element model. There are a number of experimental study outcomes to investigate on the effects of cold temperature and its applications. The material properties of steel, SUS, aluminium, and others, in particular, were studied by many researchers using experimental and numerical methods (Park et al. 2010, 2011; Yoo et al. 2011; Kim et al. 2014). They considered the effect of temperature variation and the effect of strain rate. Paik et al. (2011) performed a material coupon tensile test for ASTM A500-type carbon steel under the above-mentioned cold temperature condition by two types of cooling methods: liquid nitrogen-based cooling and dry–ice-based cooling.

Meanwhile, Park et al. (2015a) expanded experimental studies by applying various materials used in ships and offshore industry through the liquid nitrogen cooling method. This method is generally applied to investigate the effects of cold temperatures on the changes of mechanical properties. They investigated on the chemical composition and mechanical properties for various types of materials like Grade A, B, D, AH and DH grade. The aspects included yield stress, tension stress, fracture strain, behaviour of stress and strain of the material for various types of materials.

Recently, Paik et al. (2017) further investigated on the effect of strain-rate by considering the cold temperature implemented by the same testing set-up. They had established a test database of the mechanical properties of mild steel, high tensile steel, stainless steels and aluminium alloy associated with cold temperature and strain rate effect. Choi et al. (2016) also conducted material coupon test to identify the mechanical properties of high-manganese, nickel, stainless steel by considering the strain rate effect.

Table 2 shows the summary of material coupon test in cold temperature by Park et al. (2014). They had utilised the obtained material curves for assessing the structural safety of intact hull girders. In this study, the behaviour of the ultimate residual hull girder strength (or longitudinal strength) damaged by grounding in Arctic sea condition was investigated by the applied example in Section 3. The bilinear shape stress–strain curve was used in this study.

Table 2. Yield strength on different materials at cold temperatures (Park et al. 2014)

		Temperature				
Material		20°C (Room temp.)	−20°C	−40°C	−60°C	−80°C
Yield stress (σ_Y)	MS24	235.00	243.33	258.21	280.23	309.40
	HT32	315.00	315.32	323.79	337.81	357.37
	HT36	355.00	355.36	364.91	380.70	402.75

Note: unit = MPa.

2.2. Grounding damage effect

The potential risks like grounding and collision of commercial ships voyage in Arctic route should be mitigated and controlled based on proper risk management procedures. Nevertheless, there are still possibilities on grounding damage in Arctic route. It is also evident that the opportunity of Arctic route use will be increased due to global warming effects. Concomitantly, the risks of the accidental events are also increased.

Recently, Paik et al. (2012) proposed an innovative method, namely R-D diagram method to assess the structural safety of damaged structures. They verified its applicability by applying the proposed concept to the oil tankers damaged by grounding. In the similar manner, the proposed concept continued to be applied to container ships and bulk carriers (Kim et al. 2013c, 2013d).

In addition, its applicability was expanded by considering the grounding damage with time-dependent corrosion effects (Kim et al. 2014a). Initially, Paik et al. (2012) adopted modified Paik–Mansour method (Paik et al. 2013) for assessing the ultimate hull girder bending moment, while Kim et al. (2013a) compared the accuracy between modified Paik–Mansour method (Paik et al. 2013) and ALPS/HULL ISFEM (ALPS/HULL 2014) by applying the R-D diagram method.

In this study, the R-D diagram method is adopted by considering the cold temperature effect on ultimate bending moment of commercial ship voyage in Arctic sea route. It is expected that the guideline for the safety assessment of grounding damaged ship hull in Arctic sea route is going to be suggested by this study. The developed R-D diagram is to be compared by normal sea-going condition and Arctic sea-going condition.

In short, a procedure for developing the R-D diagram can be summarised, as shown in Figure 4. When the structures are characterised, the structural damage should be clearly defined in terms of damage amount, damage type, damage location and many others. In the case of grounding damage, four (4) types of damage parameters can be considered as follows.

- p_1: Grounding location in the direction of the ship's beam.
- p_2: Height of rock penetrating into the bottom of the hull in the direction of the ship's depth.
- p_3: Breadth of the bottom of the rock at the elevation corresponding to the ship's baseline and breadth of the tip of the rock.
- p_4: Angle of the rock.

Figure 4. General procedures for developing the R-D diagram and its examples (L = ship's length between perpendiculars; B = ship's breadth; D = ship's depth; b = double-side width, and h = double bottom height). (This figure is available in colour online.)

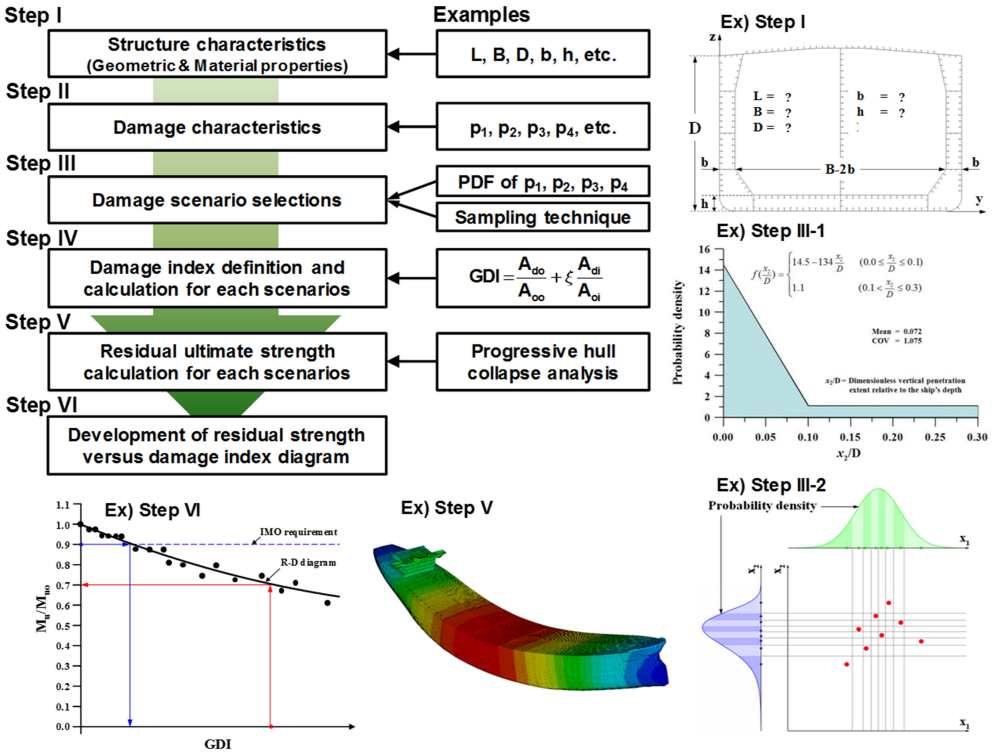

The first three (3) damage parameters (p_1,p_2 and p_3) were specified by IMO (2003) to prevent marine pollution due to grounding accidents. These provided the probability density distributions or probability density functions (PDFs), as shown in Figure A2(a) to A2(c). In the case of rock angle (p_4), 15–150 degree of the range was assumed by Paik et al. (2012), as presented in Figure A2(d). Once damage parameters were defined, the selection of reliable scenarios that can represent overall behaviour of the grounding damage accident was conducted. A large set of the scenarios may enable to produce accurate results than a limited number of dataset. It requires, however, the substantial computational cost. Concerning this, a relevant sampling technique for the section of the reliable scenario is required. In the previous study by Paik et al. (2012), Latin Hypercube Sampling (LHS) was adopted and in total, 50 cases per grounding damage scenarios were selected for numerical simulation.

The selected scenarios were then analysed by the numerical or analytical method to obtain the residual ultimate strength of damaged hull girders. In the previous study, a modified P-M method (Paik et al. 2013) had been adopted, while the ALPS/HULL ISFEM (ALPS/HULL 2014) which gave more refined results was adopted in this study. Finally, the R-D diagram was proposed based on the above-mentioned procedure in Figure 4 together with the effect of cold temperature. The cold temperature effect

in NSR was considered by changing the air temperature, as illustrated in Figure 3. It means that the material yield strength, obtained by testing illustrated in Table 2 of the outer upper side shell and the deck panel, will be changed based on assumed temperatures such as Room temperature, −20, −40, −60 and −80°C. In this study, the effect of material yield strength by low temperature is only considered, while the effect of the material toughness is not covered. Details may be referred to discussion and conclusion sections.

2.3. Method for ULS-based strength assessment

Nowadays, various types of numerical method, such as NLFEM, ISFEM, ISUM or Smith method, are adopted for the safety assessment in the field of ships and offshore construction industries. The analytical method and empirical formulation (or closed form shape design formula) are also considered as the efficient methods to evaluate the hull girder structural safety in a short period of time. In the case of a structural analysis method, a number of benchmark studies were performed previously to identify the accuracy of each method in comparison to the experimental results. In the case of the experimental method, Dow (1991) performed a progressive hull girder collapse analysis for 1/3-scale frigate test hull. After his experiment, a number of comparison studies were conducted (Paik and Mansour 1995 **[Q4]**; Gordo and Guedes Soares 1996; ISSC 2012; Paik et al. 2013) and Yao (2003) reviewed various types of approaches and their results.

ISSC (2009, 2012, 2015, 2018) conducted a wide range of benchmark and parametric studies to evaluate the accuracy of existing methods by adopting numerical and analytical methods. In the case of ultimate strength of hull girder, ISSC (2012) conducted benchmark studies for selected six (6) ship hulls by adopting the abovementioned methods. Such methods include numerical methods like NLFEM (ANSYS 2012), ISEFM (ALPS/HULL 2014), ISUM (Kim et al. 2013b), and analytical method (Paik et al. 2013) for the comparison purpose.

In the present study, one of the numerical methods, ALPS/HULL ISFEM, was adopted for the progressive hull girder collapse analysis under cold temperature. This method was also applied for assessing the ultimate limit state of the intact and damaged hull girders (Paik et al. 2009; Kim et al. 2012b, 2012c, 2014b, 2015) and compared with other analytical and FE methods (Kim et al. 2013a, 2013c). The typical modelling of the Panamax class double hull oil tanker using ALPS/HULL software is shown in Figure 5. The accuracy of this method had been verified by ISSC (2012) and Paik (2018). The details of ALPS/HULL progressive hull girder collapse analysis programme may be referred to Hughes and Paik (2010).

Figure 5. A typical model for Panamax class double hull oil tanker by ISFEM (ALPS/HULL 2014). (This figure is available in colour online.)

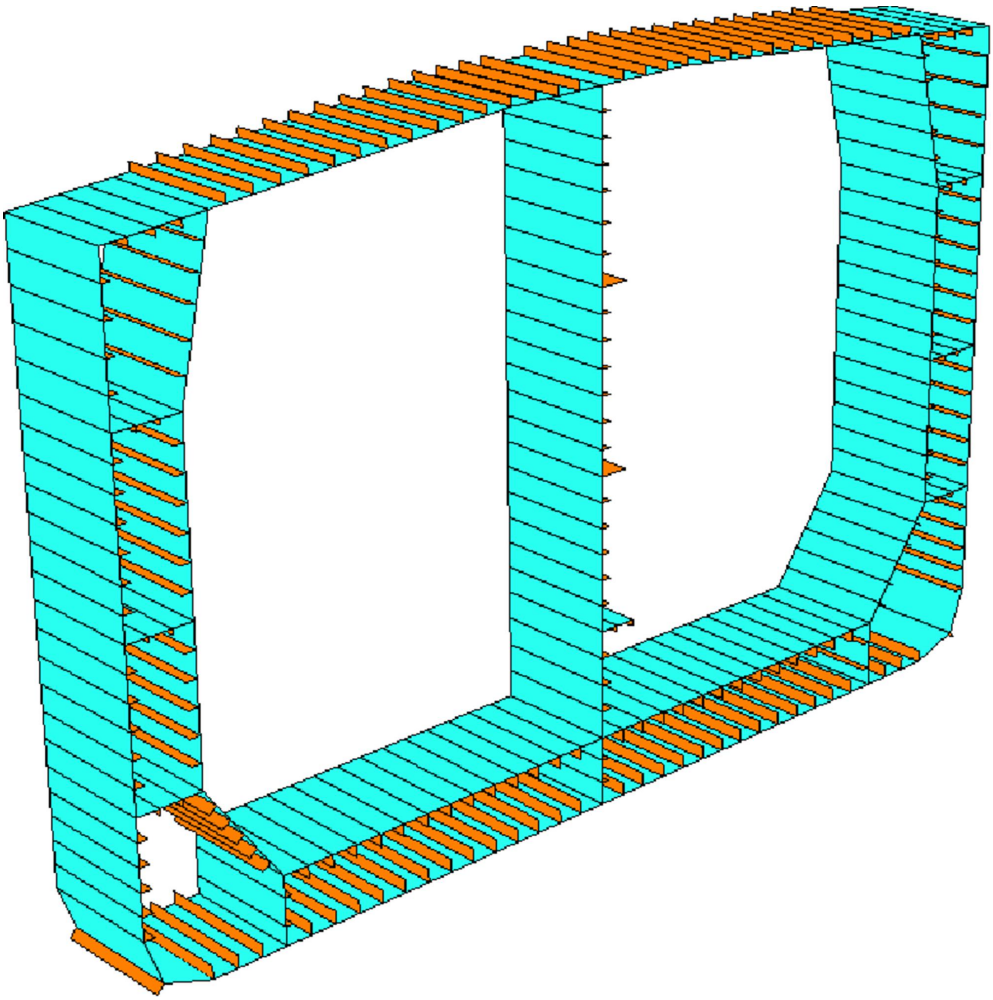

2.4. Assumption and limitation of the present study

In the present study, a useful diagram to assess the safety of grounded ships in NSR will be proposed. It means that the effect of cold temperature and grounding damage of the ship structure can be covered by the proposed diagram. In this section, the assumption and the limitation will be addressed as follows. The details will be recapped in the conclusion section.

Figure 6. (a) Designs of target structure (Note: IS = inner shell, OS = outer shell, H = hopper, IB = inner bottom, OB = outer bottom, CBH = centre bulk head, CL = centre line). (b) Application of cold temperature to the target structure (Park et al. 2014). (This figure is available in colour online.)

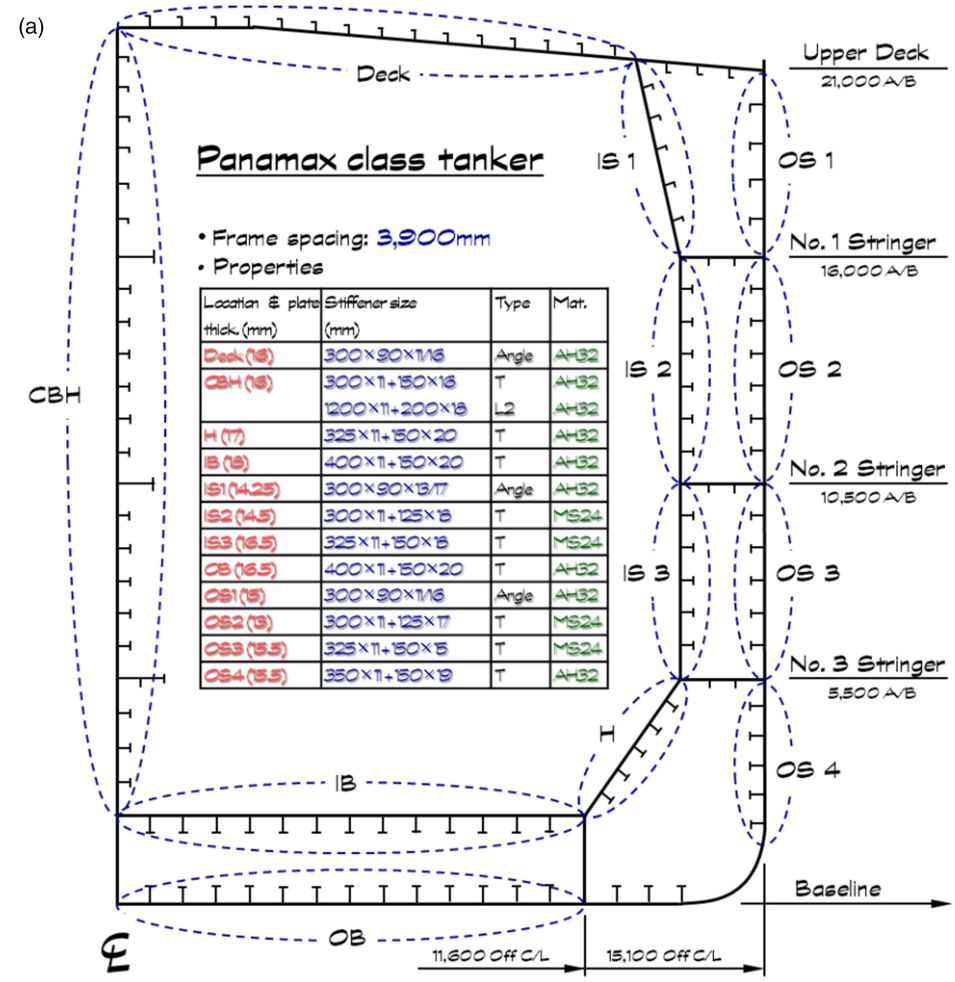

Location & plate thick. (mm)	Stiffener size (mm)	Type	Mat.
Deck (18)	300×90×11/16	Angle	AH32
CBH (18)	300×11+150×16	T	AH32
	1200×11+200×18	L2	AH32
H (17)	325×11+150×20	T	AH32
IB (18)	400×11+150×20	T	AH32
IS1 (14.25)	300×90×13/17	Angle	AH32
IS2 (14.5)	300×11+125×18	T	MS24
IS3 (16.5)	325×11+150×18	T	MS24
OB (16.5)	400×11+150×20	T	AH32
OS1 (15)	300×90×11/16	Angle	AH32
OS2 (13)	300×11+125×17	T	MS24
OS3 (15.5)	325×11+150×15	T	MS24
OS4 (15.5)	350×11+150×19	T	AH32

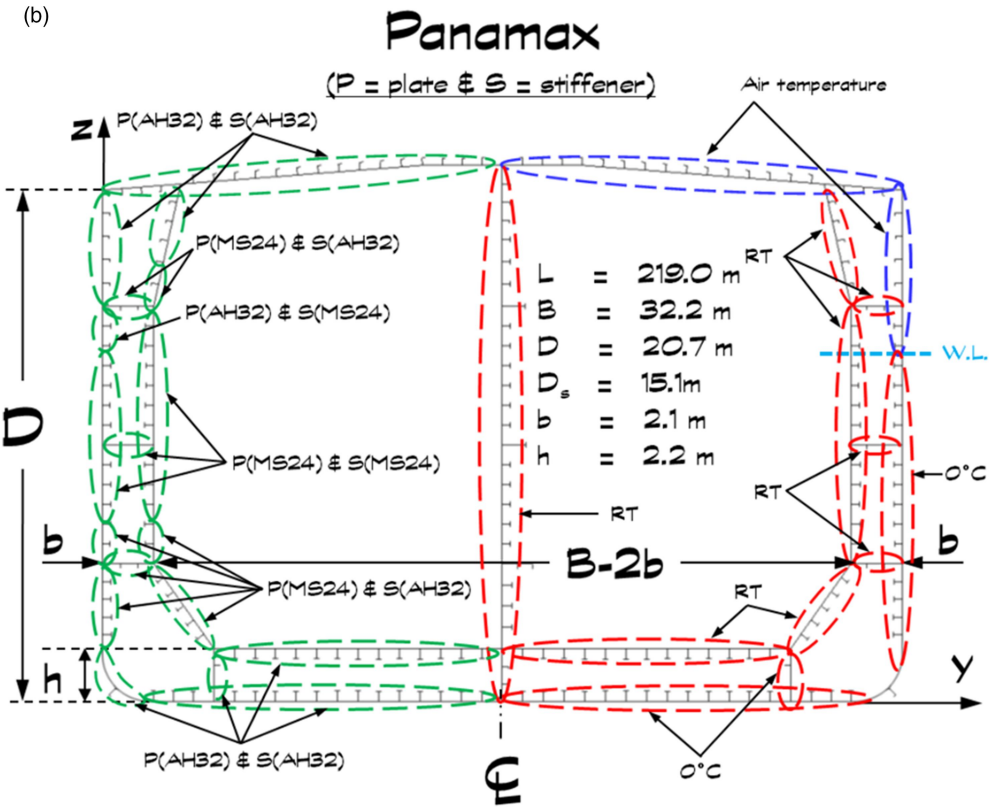

- The present study only considered the grounded commercial ships constructed for voyage in South Sea Route (SSR).
- The considered loads are only vertical bending moments such as hogging and sagging condition.
- The considered air temperature range in NSR is from room temperature to −80°C. Details may be referred to Table 2 and temperature application can also be found in Figure 6.
- The water folding effect and the rotation of the hull girder by grounding damage were not considered in this study

(The vessel was kept on the upright condition after the grounding damage). In this regard, the rotation of neutral axis may be recommended to be conducted in the near future.

- In the case of material property, bilinear type stress–strain curve with no tangential angle has been adopted. The only mechanical consequence of the low temperature in the present paper is the yield strength while strain effect, i.e. material toughness, was not considered. It means that selected vessel was designed for voyage through SSR and was applied to NSR to investigate its applicability by applying different surrounded air temperature which may change the material yield strength and material toughness.
- For the consideration of grounding damage, structural element removal method has been applied. It means that the effect of local plastic deformation can be neglected.
- For the calculation of ultimate hull girder strength of grounded ship, ALPS/ULSAP ISFEM was adopted by using bilinear curve stress–strain curve (The accuracy of this software is verified by ISSC (2012) and Kim et al. (2013) **[Q5]**).
- The applied modelling techniques, i.e. element removal method and bilinear stress–strain curve with no tangential angle, may underrate the residual ultimate hull girder strength of ships under grounding damage. However, it may help the robust design of ship's hull by considering safety margins.

3. Applied examples

In this section, an R-D diagram for vessels traversed through NSR damaged by grounding was proposed based on the given procedure in Figure 4.

3.1. Target structure

In the case of vessel voyage in NSR, its beam (breadth) cannot exceed the 30 m as vessel should not be wider than the ice-breaking ship (Ragner 2008). In this regard, Panamax class double hull oil tanker, which was the most suitable and smallest oil tanker to pass through the Suez Canal, was selected as the target structure in this study. Currently, the Post-Panamax class (maximum breadth = 49 m) is able to operate. The details of the commercial Arctic shipping through the NSR in terms of routes, resources, governance, technology and infrastructures may be referred to Farré et al. (2014). In this study, the smallest vessel among the oil tankers was selected as the target structure, as shown in Figure 6. It shows the midship section of the Panamax class double hull oil tanker with the principal dimensions of the ship (L = 219 m, B = 32.2 m, D = 20.7 m). The breadth was slightly wider than the expected size (30 m). However, it was assumed to be within the considerable range in this study for the application. The geometric and material properties of mid-ship section, including plate and stiffener, are presented in Figure 6(a) and cross-sectional data of target structure are summarised in Table 3. The application of the cold temperature is also presented in Figure 6(b).

Table 3. Cross-sectional data of the target structure.

Ship type	A (m^2)	I (m^4)		N.A. (m)
		Vertical	Horizontal	
Panamax class tanker	4.523	276.637	576.434	9.099

3.2. Consideration of grounding damages on Panamax class oil tanker under Arctic condition

The structural characteristics are identified in Figure 6. The characteristics of grounding damage (i.e. p_1, p_2, p_3 and p_4) and damage scenario selections were performed based on the defined structural characteristics. The selected damage scenarios are presented in Table 4. In total, fifty (50) grounding damage scenarios selected are shown in Table 4 for the residual ultimate hull girder strength analysis as well as definition of grounding damage index (GDI).

Table 4. The selected damage scenarios with damage parameters (Paik et al. 2012).

Scenario	p_1	p_2	p_3	p_4
1	0.010B	0.080D	0.144B	103.0
2	0.030B	0.017D	0.918B	88.3

3	0.050B	0.071D	0.064B	56.2
4	0.070B	0.019D	0.018B	124.0
5	0.090B	0.200D	0.777B	101.3
6	0.110B	0.016D	0.008B	74.0
7	0.130B	0.026D	0.945B	80.6
8	0.150B	0.182D	0.127B	116.5
9	0.170B	0.273D	0.427B	84.4
10	0.190B	0.219D	0.046B	96.6
11	0.210B	0.109D	0.195B	71.3
12	0.230B	0.044D	0.090B	81.9
13	0.250B	0.011D	0.023B	72.7
14	0.270B	0.008D	0.083B	99.7
15	0.290B	0.291D	0.013B	62.0
16	0.310B	0.024D	0.104B	79.3
17	0.330B	0.075D	0.327B	51.4
18	0.350B	0.033D	0.034B	53.9
19	0.370B	0.052D	0.058B	48.5
20	0.390B	0.040D	0.477B	138.7
21	0.410B	0.042D	0.577B	93.7
22	0.430B	0.255D	0.070B	87.0
23	0.450B	0.067D	0.980B	26.2
24	0.470B	0.004D	0.237B	106.7
25	0.490B	0.028D	0.003B	85.7
26	0.510B	0.049D	0.183B	92.3
27	0.530B	0.095D	0.377B	63.7
28	0.550B	0.005D	0.827B	111.1
29	0.570B	0.021D	0.153B	113.6
30	0.590B	0.038D	0.052B	75.4
31	0.610B	0.128D	0.877B	60.2
32	0.630B	0.057D	0.994B	83.1
33	0.650B	0.086D	0.097B	41.0
34	0.670B	0.006D	0.257B	89.6
35	0.690B	0.164D	0.221B	78.0

36	0.710B	0.022D	0.135B	66.9
37	0.730B	0.060D	0.727B	119.8
38	0.750B	0.036D	0.162B	76.7
39	0.770B	0.064D	0.076B	58.2
40	0.790B	0.032D	0.207B	68.4
41	0.810B	0.002D	0.119B	95.1
42	0.830B	0.014D	0.677B	98.1
43	0.850B	0.146D	0.111B	65.3
44	0.870B	0.012D	0.964B	129.8
45	0.890B	0.030D	0.040B	35.2
46	0.910B	0.047D	0.527B	104.8
47	0.930B	0.009D	0.029B	108.8
48	0.950B	0.237D	0.627B	69.9
49	0.970B	0.001D	0.172B	45.2
50	0.990*B*	0.054D	0.285B	91.0

Note: P_1 = Grounding location in the direction of the ship's beam; P_2 = Height of rock penetrating into the bottom of the hull in the direction of the ship's depth; P_3 = Breadth of the bottom of the rock at the elevation corresponding to the ship's baseline and breadth of the tip of the rock; P_4 = Angle of the rock; B = Ship's breadth; and D = Ship's depth.

As mentioned earlier, the PDFs of damage parameters, i.e. grounding location (p_1), height of rock penetrating into the bottom (p_2) and breadth of the bottom of the rock (p_3), were specified and provided by IMO (2003), as shown in Figure A2(a) to A2(c). In the case of rock angle (p_4), 15–150 degree of the range was assumed by Paik et al. (2012), as presented in **[Q8]** Figure A4(d). Based on defined grounding damage parameters and PDFs, the probability (P) of each of M samples generated by the LHS technique for N variables could be obtained by $P = \left(\frac{1}{M}\right)^N$. In this way, fifty (50) reliable grounding damage scenarios were selected by a combination of damage parameters ($p_1 - p_4$) by the LHS technique.

3.3. Calculation of GDI

Prior to performing the residual ultimate strength analysis, damage index was defined and calculated. Equation (1) shows the definition of the damage index for grounded ships by Paik et al. (2012).

$$\mathrm{GDI} = \frac{A_{\mathrm{ro}}}{A_{\mathrm{oo}}} + \xi \frac{A_{\mathrm{ri}}}{A_{\mathrm{oi}}} \qquad (1)$$

where A_{oi} = original cross-sectional area of the inner bottom, A_{oo} = cross-sectional area of the OB, A_{ri} = reduced (damaged) cross-sectional area of the inner bottom, A_{ro} = reduced (damaged) cross-sectional area of the OB.

Intact and damaged areas can be simply calculated from the formula. The correction factor (ξ) can be defined as a ratio of the variation in ultimate hull girder (or longitudinal) strength between the outer and inner bottom structures, as shown in Equation (2). In this regard, the correction factor can present the contribution of the cross-sectional area of the inner bottom to the ultimate hull girder strength performance, as shown in Equation (2). Therefore, the deduction of the cross-sectional area of the inner bottom (IB) does not include the OB damage. This is for the calculation of the contribution from the IB and OB to the deduction of ultimate longitudinal strength, separately.

$$\zeta = \frac{\theta_{IB}}{\theta_{OB}} \qquad (2)$$

where, θ_{OB} and θ_{IB} = slopes of the ultimate hull girder strength and the amount of grounding damage area for the outer and inner bottom panels, respectively.

Figure 7(a) represents the variation in Mu/Muo for the selected Panamax class double hull oil tanker in a hogging and sagging condition as the amount of damage in the outer and inner bottom increases, where Mu and Muo represent the ultimate longitudinal strength (or ultimate hull girder strength) of the damaged ship at different temperatures (i.e. Room temp. to −80°C) and intact ship at room temperature, respectively.

Figure 7. Determination of the correction factors. (a) Typical example of the correction factor at −20°C. (b) Correction factor versus temperature. (This figure is available in colour online.)

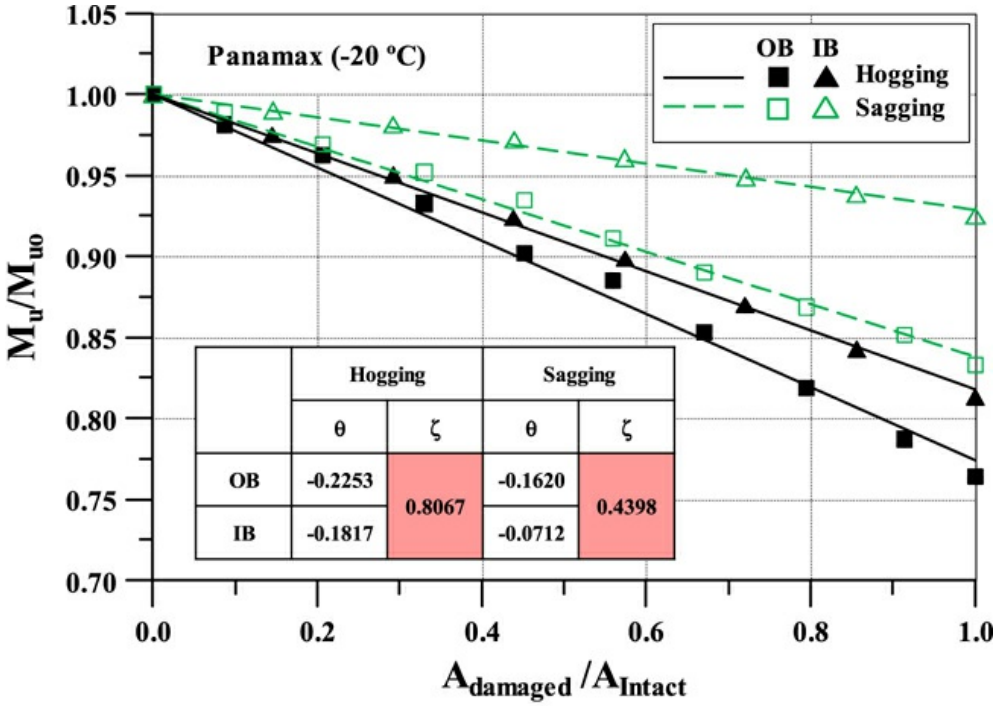

(a)

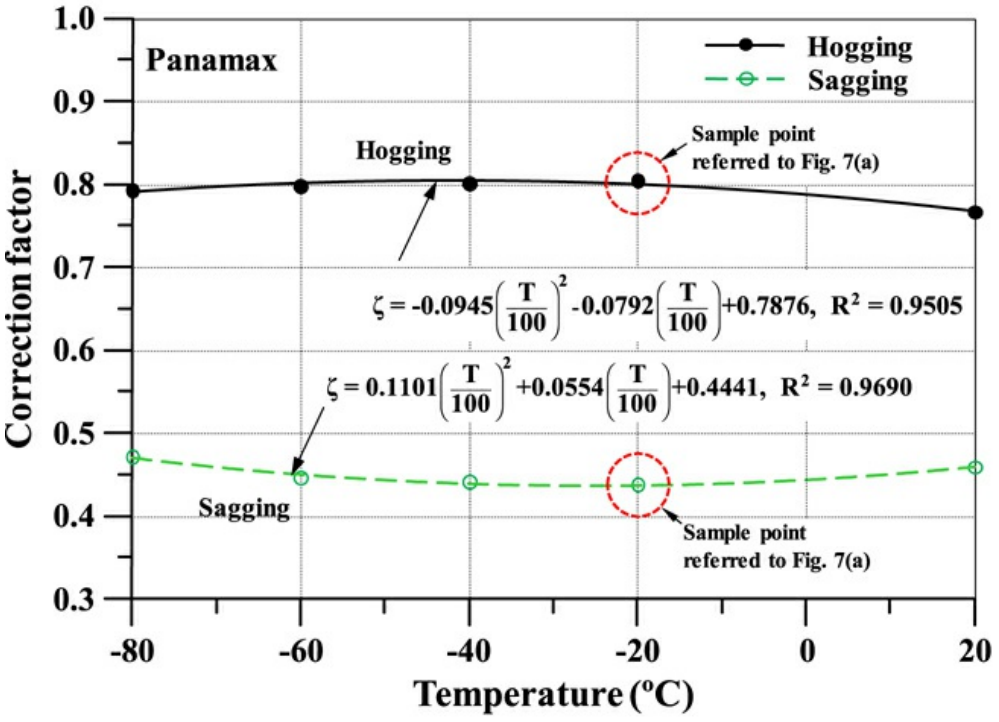

(b)

Figure 7(a) shows the typical example to obtain the correction factor (ξ) at −20°C. The residual ultimate hull girder strength was plotted as a function of grounding damage amount. The effect of area deduction in the OB and the inner bottom by considering the increased grounding damage was investigated under hogging and sagging bending moments. In total, four (4) straight lines with slopes (θ_{OB} and θ_{IB}) were obtained by linear curve fitting based on the obtained analysis results. The correction factors (ξ) in hogging and sagging were 0.8067 and 0.4398, respectively.

In the same manner, correction factors in different temperature were obtained and plotted in Figure 7(b). As mentioned before, the obtained correction factors, 0.8067 and 0.4398, were plotted to represent the temperature of −20°C. Based on the obtained correction factor values, empirical formulation to predict correction factor under hogging and sagging bending moments was proposed by curve fitting, as shown in Figure 7(b). The GDI can then be finally defined by Equation (1), while the proposed correction factor (ξ) by curve-fitting shape is shown in Figure 7(b).

$$\xi = \begin{cases} 0.1101\left(\frac{T}{100}\right)^2 + 0.0554\left(\frac{T}{100}\right) + 0.4441 \text{ in Sag} \\ -0.0945\left(\frac{T}{100}\right)^2 - 0.0792\left(\frac{T}{100}\right) + 0.7876 \text{ in Hog} \end{cases} \quad (3)$$

where T = temperature (°C).

The obtained outcome was very useful to determine a correction factor by empirical formulation in Equation (3) for the Arctic sea condition.

3.4. Calculation of the residual strength

The residual ultimate hull girder strengths of fifty (50) grounding damage scenarios of Panamax class double hull oil tanker were computed by ALPS/ULSAP ISFEM, as shown in Figure 8(a–e). The damaged structural element by grounding accident was removed where the negative contribution of the damaged structural members was assumed.

Figure 8. The obtained R-D diagrams for Panamax class double hull oil tanker. (a) Room temperature condition. (b) −20°C condition. (c) −40°C condition. (d) −60°C condition. (e) −80°C condition. (This figure is available in colour online.)

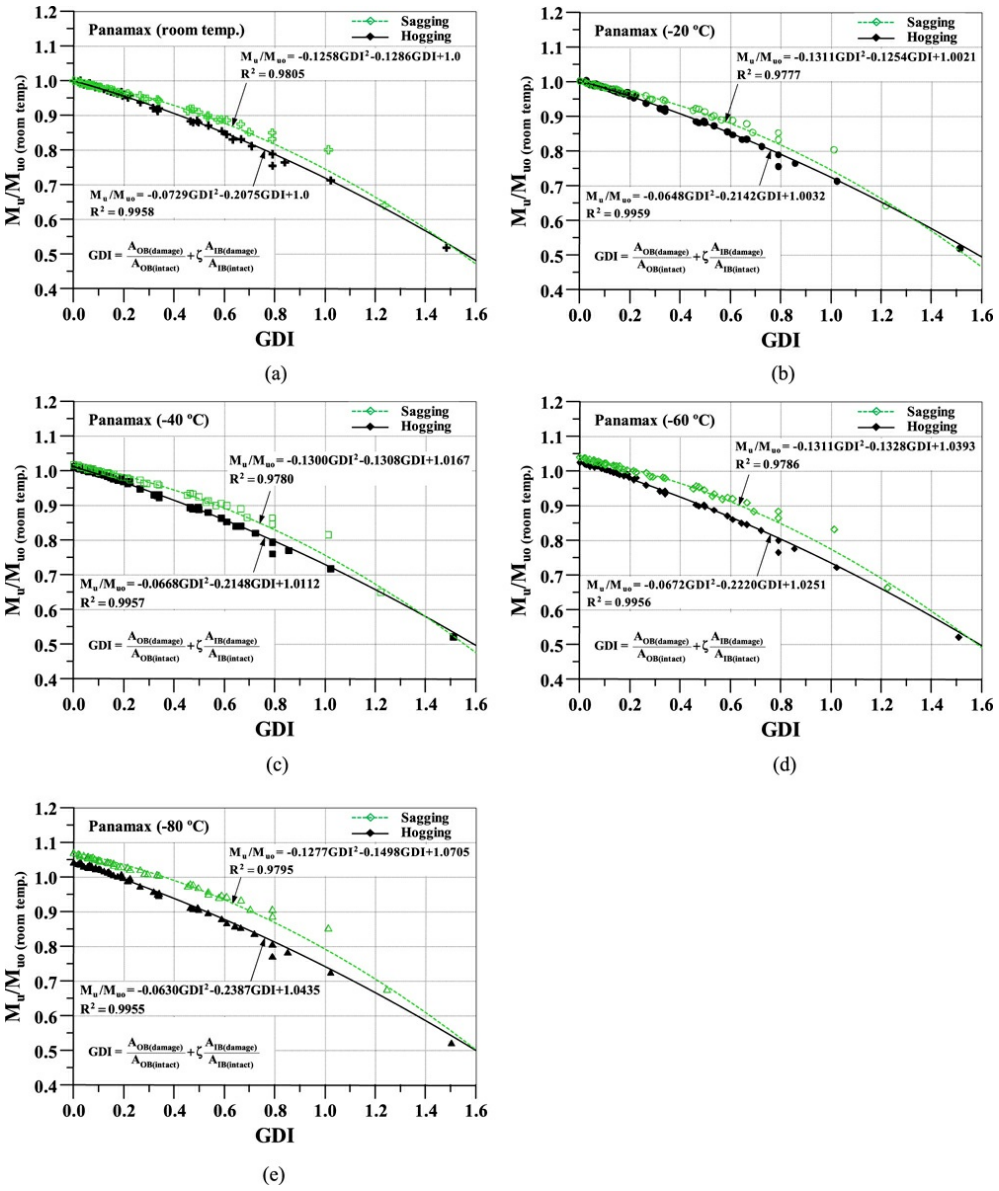

3.5. Development of R-D diagram considering the cold temperature

The fifty (50) grounding damage scenarios with five (5) temperatures under two (2) types of VBMs (i.e. hogging and sagging bending moments) were considered to calculate residual ultimate hull girder strengths. Those temperatures were RT, −20°C, −40°C, −60°C and −80°C. In total, the 500 cases of the residual ultimate hull girder strengths were plotted based on the determined GDI in Figure 8(a–e). The obtained R-D diagrams for each of the five (5) temperatures by curve-fitting were presented with computation results.

As expected, single representative empirical formulation could be obtained with higher accuracy (R^2 = above 0.97). The R-D diagrams behave differently with the loading conditions such as hogging and sagging bending moments. The empirically formulated R-D diagrams based on the temperature are summarised in Equations (4a)–(4e).

R-D diagram at RT

$$\frac{M_u}{M_{uo}} = \begin{cases} -0.0729\,GDI^2 - 0.2075\,GDI + 1.0 \ \text{ in Hogging} \\ -0.1258\,GDI^2 - 0.1286\,GDI + 1.0 \ \text{ in Sagging} \end{cases} \quad (4a)$$

R-D diagram at −20°C

$$\frac{M_u}{M_{uo}} = \begin{cases} -0.0648\,GDI^2 - 0.2142\,GDI + 1.0032 & \text{in Hogging} \\ -0.1311\,GDI^2 - 0.1254\,GDI + 1.0021 & \text{in Sagging} \end{cases} \quad (4b)$$

R-D diagram at −40°C

$$\frac{M_u}{M_{uo}} = \begin{cases} -0.0668\,GDI^2 - 0.2148\,GDI + 1.0112 & \text{in Hogging} \\ -0.1300\,GDI^2 - 0.1308\,GDI + 1.0167 & \text{in Sagging} \end{cases} \quad (4c)$$

R-D diagram at −60°C

$$\frac{M_u}{M_{uo}} = \begin{cases} -0.0672\,GDI^2 - 0.2220\,GDI + 1.0251 & \text{in Hogging} \\ -0.1311\,GDI^2 - 0.1328\,GDI + 1.0393 & \text{in Sagging} \end{cases} \quad (4d)$$

R-D diagram at −80°C

$$\frac{M_u}{M_{uo}} = \begin{cases} -0.0630\,GDI^2 - 0.2387\,GDI + 1.0435 & \text{in Hogging} \\ -0.1277\,GDI^2 - 0.1498\,GDI + 1.0705 & \text{in Sagging} \end{cases} \quad (4e)$$

As presented in Table 2, the material yield strength (σ_Y) increased as the temperature decreased. The same trend had been observed in residual ultimate hull girder strength obtained by numerical simulation in this study, as shown in Figure 9(a,b). In this section, the R-D diagram, as a shape of empirical formulation by curve-fitting, was developed for assessing the safety of the grounded ship in NSR by considering the cold temperature effect.

Figure 9. The trend of residual ultimate hull girder strength by grounding damage and temperature. (a) Sagging condition (b) Hogging condition. (This figure is available in colour online.)

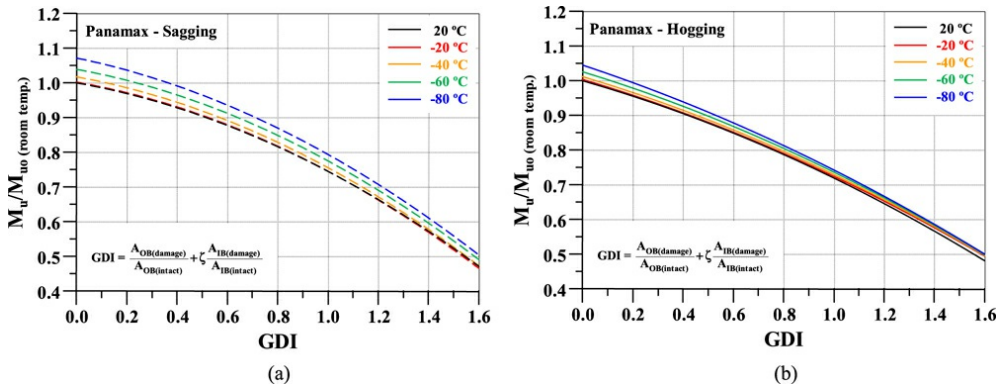

3.6. Consideration of the effect of temperatures

Based on the obtained empirical formulations (R-D diagram) as shown in Figure 8, an additional correction factor to consider the effect of temperature was investigated. The obtained R-D diagram at RT (20°C) was set as the reference data and the difference was investigated, as shown in Figures 10 and 11 for the consideration of sagging and hogging condition, respectively. The correction factor for considering the temperature variation is presented in Equation (5).

$$c_T = \begin{cases} -31.472\left(\frac{T}{1000}\right)^3 + 6.5551\left(\frac{T}{1000}\right)^2 - 0.1042\left(\frac{T}{1000}\right) \\ \quad +1.0002 \text{ for sagging} \\ 8.6671\left(\frac{T}{1000}\right)^3 + 3.2936\left(\frac{T}{1000}\right)^2 - 0.19821\left(\frac{T}{1000}\right) \\ \quad +1.0026 \text{ for hogging} \end{cases} \quad (5)$$

where c_T = correction factor for considering temperature variation, T = temperature (Note: the temperature in NSR from RT to −80 can only be applied).

Figure 10. The effect of temperature on the difference of the R-D diagram. (a) Sagging condition. (b) Hogging condition. (This figure is available in colour online.)

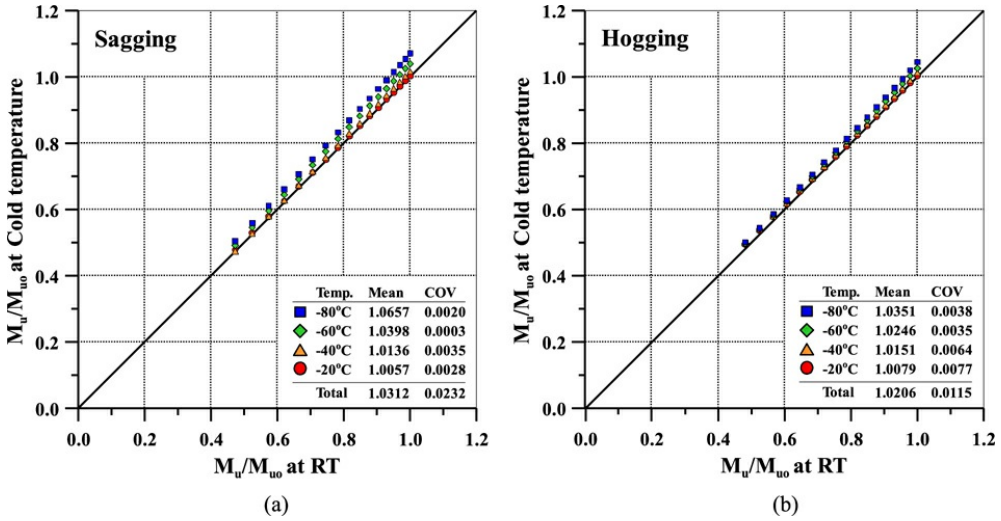

Figure 11. The effect of temperature on the difference of the R-D diagram in hogging condition. (This figure is available in colour online.)

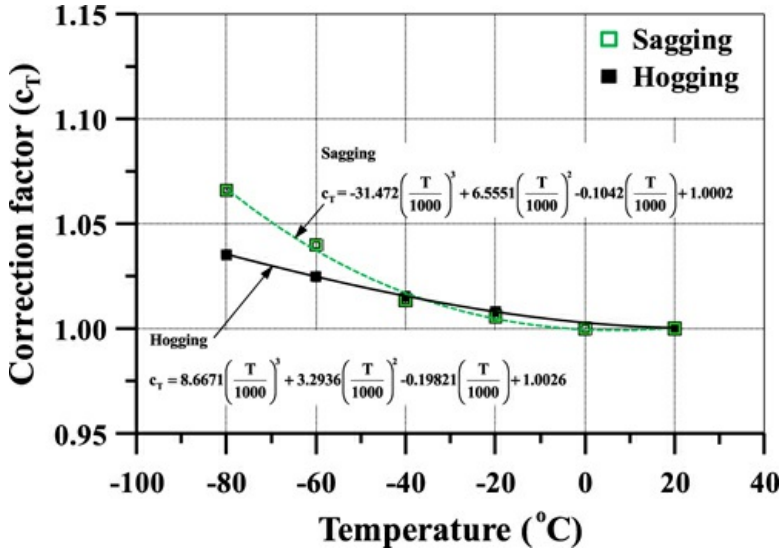

From the investigation, it was found that the difference of the R-D diagram between RT and other cold temperatures (−20°C, −40°C, −60°C and −80°C) had a linear relationship. It means that the difference can be investigated and represented by mean values, as shown in Figure 10(a,b) for sagging and hogging condition, respectively. The obtained mean values represent the increment of the ultimate longitudinal strength of hull girder. The relationship between mean value and temperature is formulated by curve-fitting, as shown in Equation (5) and Figure 11.

As would be expected, well-fitted correction factors for sagging and hogging conditions are obtained as a shape of empirical formulation by curve-fitting, as shown in Figure 11. Therefore, the modified R-D diagram can then be proposed, as shown in Equation (6). Finally, the original R-D diagrams, shown in Equation (1) and the modified R-D diagrams, by considering the temperature variation coefficient in Equation (6) were compared in Figure 12.

Figure 12. The correction factor to consider the effect of temperature. (a) in sagging. (b) in hogging. (This figure is available in colour online.)

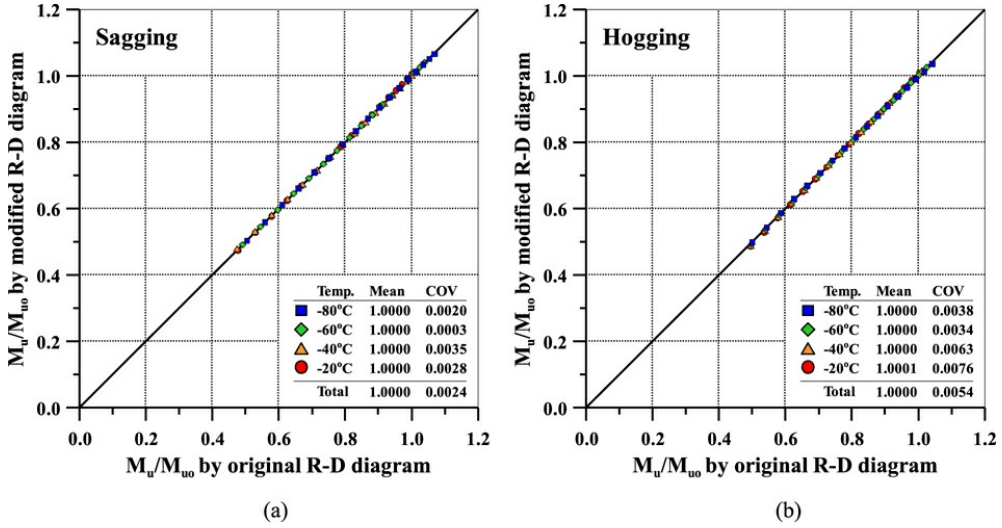

From the statistical analysis in Figure 12(a,b), the differences between original and the modified R-D diagrams were investigated by Mean (=1.0000 for both sagging and hogging condition, respectively) and coefficient of variation values (=0.0024 and 0.0054 for sagging and hogging condition, respectively). It is concluded that the accurate and reliable results can be obtained by the proposed modified R-D diagram, as shown in Equation (6).

$$\frac{M_{\mathrm{u}}}{M_{\mathrm{uo}}} = \begin{cases} c_T(-0.1258\mathrm{GDI}^2 - 0.1286\mathrm{GDI} + 1.0) & \text{in sagging} \\ c_T(-0.0729\mathrm{GDI}^2 - 0.2075GDI + 1.0) & \text{in hogging} \end{cases} \tag{6}$$

where c_T = correction factor for considering temperature variation illustrated in Equation (5), GDI = grounding damage index presented in Equation (1).

The final outcomes shown in Equation (6) can be used by following steps.

[Step 1] Calculation of grounding damage index (GDI) by defining the grounding damage amount

[Step 2] Calculation of c_T from the given Equation (5)

[Step 3] Substitution of the calculated GDI and c_T to Equation (6)

[Step 4] Calculation of ultimate bending moment and assessment of the safety based on safety criteria (In this study, M_u/M_{uo} = 0.9 is set as safety criterion, as shown in Figure 13)

Figure 13. The use of the obtained R-D diagram. (This figure is available in colour online.)

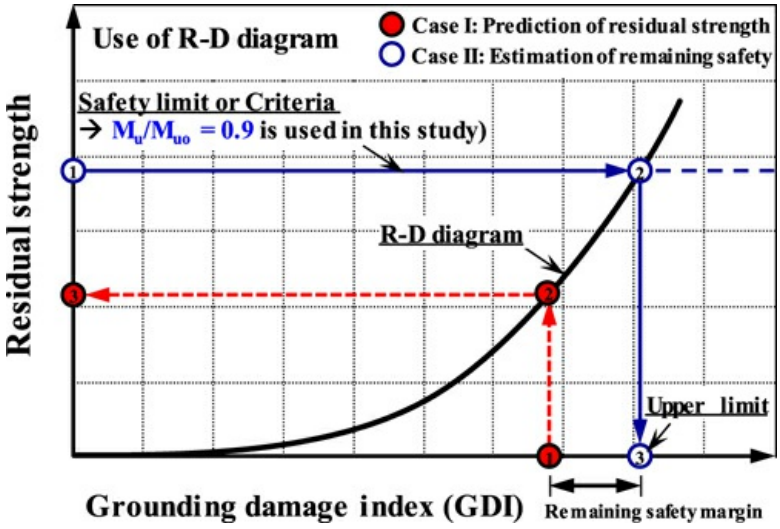

3.7. Discussion on the possible uses of the obtained R-D diagrams

In this section, the R-D diagram was used for assessing the safety of the grounded ship in NSR. Figure 13 represents a schematic view of the R-D diagram. It shows that when the GDI is calculated, the ratio of residual ultimate hull girder strength (M_u/M_{uo}) can be simply obtained from the R-D diagram. That is represented as case I in Figure 13. In the case of GDI, it can be computed by using Equations (1) and (3) by identifying the damage location, amount and the correlation between damage in the outer and inner bottoms.

At the same time, the remaining safety margin or safety level can also be obtained if there is a clear guideline for safety limitations or safety criteria. For example, IMO (2000) proposed that the vessel's hull girder strength was not reduced up to 10% compared with as-built condition. It means that the damaged ship should maintain 90% or above 90% of the residual strength. Therefore, $M_u/M_{uo} = 0.9$ can be set as the safety limit in the given R-D diagrams so that the upper limit of GDI can then be obtained, as shown in Figure 13 (Case II). The remaining safety margin can be defined as a function of GDI by using the distance between the upper limit and calculated values of GDI.

In this way, the upper limits of the GDI correspond to the 90% of the ultimate hull girder strength in an as-built condition specified by IMO (2000). These are computed and summarised in Table 5. The upper limit of the GDI is formulated in Equation (7) as a shape of empirical formulation based on data shown in Table 5. The trend of the upper limit of GDI can be referred to Figure 14. In the previous study, Paik et al. (2012) had observed that the upper limit of GDI decreased for both sagging and hogging conditions, as vessel size increased. They had considered four (4) different sizes of the double hull oil tankers. In this study, we had observed that the upper limit of GDI decreased for both sagging and hogging conditions as the temperature increased. On the other hand, the decreasing trend of the upper limit of GDI was faster in hogging than sagging condition.

Figure 14. The upper limit of GDI. (This figure is available in colour online.)

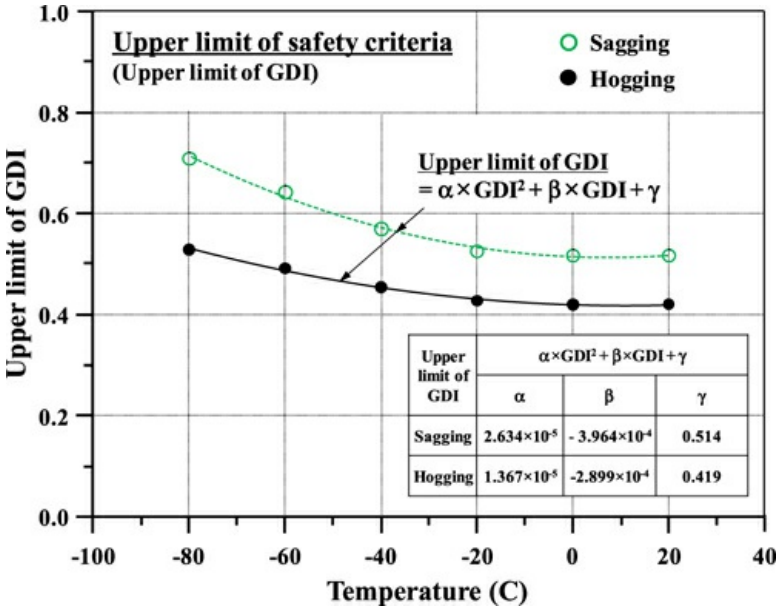

Table 5. Upper limit of the GDI for assessing the remaining safety of grounding damaged ships.

Temp.	20°C	0°C	−20°C	−40°C	−60°C	−80°C
Sagging	0.5166	0.5166	0.5255	0.5697	0.6420	0.7093
Hogging	0.4200	0.4200	0.4267	0.4537	0.4906	0.5277

This phenomenon can be easily understood by considering the damage location due to grounding accident. The structural members in the bottom part, which were located far from the neutral axis contributed to resist the longitudinal compression. They played their roles when the vertical hogging bending moment was applied to the ship or ship-shaped offshore structures. The loss of the structural elements in the bottom part, i.e. plates and stiffeners, by grounding accident may lead to the deduction of the structural capacity to resist compression in the bottom caused by the vertical hogging bending moment. While the structural elements in deck part will not be damaged by grounding accident, the vertical sagging bending moment capacity will remain higher than the hogging condition.

Upper limit of the GDI

$$GDI_{\text{upper limit}} = \begin{cases} 2.634 \times 10^{-5} GDI^2 - 3.964 \times 10^{-4} GDI + 0.514 \text{ in Sagging} \\ 1.367 \times 10^{-5} GDI^2 - 2.899 \times 10^{-4} GDI + 0.419 \text{ in Hogging} \end{cases} \quad (7)$$

4. Conclusions

Since the early twenty-first Century, the effects of global warming were greatly highlighted. Especially in 2018, it was reported that several countries were experiencing the abnormal climate due to global warming. However, it may have opened up the new opportunities for the commercial voyage in NSR during the summer season. Moreover, it was reported that the NSR may have reduced the navigational distance between Asia and Europe by about 40%.

By considering the abovementioned situations, a R-D diagram was proposed for assessing the safety of the ships grounded in NSR. The obtained outcomes are summarised as follows.

- A useful diagram (R-D diagram) was proposed to be used for the structural safety assessment of commercial ship damaged by grounding in NSR by considering cold temperatures (RT, −20°C, −40°C, −60°C and −80°C).
- The reliable grounding damage scenarios were considered for the development of R-D diagram.
- It was as expected that, as grounding damage was increased, the ultimate longitudinal strength of the ship's hull damaged by grounding was decreased. The trend was presented by the R-D diagram.
- As the temperature decreased, the material yield strength increased (as shown in Table 2). In the same manner, the trend of the ultimate longitudinal strength behaviour of the hull girder damaged by grounding increased as the temperature decreased. The cold temperature effect could be presented by adopting the correction factor, as shown in Figure 12.
- As the temperature increased, the upper limit of GDI decreased for both sagging and hogging conditions. In contrast, the decreasing trend of the upper limit of GDI was faster in hogging than in sagging condition.
- A meaningful user manual is provided in Figure 13 for a quick and accurate assessment of structural safety of grounding damaged ship in NSR.

The present study only considered the grounded commercial ships under the vertical sagging and hogging bending moments. However, the water flooding effect and rotation of the hull girder were not considered. It means that the vessel was kept on the upright condition after the grounding accident occurred. The rotation of the neutral axis may also be considered in the near future. From this study, it is confirmed that the proposed R-D diagram concept can be applied to various types of damaged structures, and the other effect (low temperature effect) may also be adopted.

In addition, the only mechanical consequence of the low temperature in the present paper is the yield strength, while strain effect, i.e. material toughness, was not considered. It means that selected vessel was designed for voyage through SSR and was applied to NSR to investigate its applicability by revising surrounded air temperature which may change the material yield strength and material toughness. However, the effect of material yield strength by low temperature is only considered in the present study. It is also to be noted that classification societies in their rules propose steel of improved toughness for cold regions

such as Grade B, D, E and F.

The obtained outcome may be applied to assessing the structural safety of the ship's hull girder constructed by Grade A steel grounded in NSR. In addition, the proposed diagram may be used to determine the acceptance criteria (upper limit of GDI as shown in Figure 14) for a for residual strength performance associated with certain amounts of grounding damage. Further studies are being carried out to propose a new R-D diagram for assessing the structural safety of the ship's hull collided in normal and cold temperatures.

Disclosure statement

No potential conflict of interest was reported by the authors **[Q6]**.

ORCID

Do Kyun Kim http://orcid.org/0000-0001-5735-4625

Jeom Kee Paik http://orcid.org/0000-0003-2956-9359

References

ALPS/HULL. 2014. A computer program for progressive collapse analysis of ship hulls. Stevensville, MD: Advanced Technology Center, DRS C3 Systems, Inc. Available from: http://www.proteusengineering.com, www.maestromarine.com.**[Q7]**

ANSYS. 2012. Version 13.0. Canonsburg, PA: ANSYS Inc.

Choi HS, Shin G, Choung JM, Kim KH, Seo DW, Kim KS, Wong EWC, Kim DK. 2016. Applicability of high manganese steel to FLNG storage tank considering collision damage. The International Conference on Ocean, Mechanical and Aerospace for Scientists and Engineer (OMAse 2016), 7–8 November; Terengganu, Malaysia.

ChosunBiz. 2012. The collapse of the Pacific Carrier by Typhoon Bolaven at Sacheon. Seoul: ChosunBiz Newspaper (in Korean Language).

Dow RS. 1991. Testing and analysis of a 1/3-scale welded steel frigate model. The 2nd International Conference on Advances in Marine Structures, 21–24 May; Dunfermline, Scotland.

Emmerson C, Lahn G. 2012. Arctic opening: opportunity and risk in the high north. London: Lloyd's, Chatham House.

Farré AB, Stephenson SR, Chen L, Czub M, Dai Y, Demchev D, Efimov Y, Graczyk P, Grythe H, Keil K, et al. 2014. Commercial Arctic shipping through the Northeast Passage: routes, resources, governance, technology, and infrastructure. Polar Geogr. 37(4):298–324.

Gordo JM, Guedes Soares C. 1996. Approximate method to evaluate the hull girder collapse strength. Marine Struct. 9(3–4):449–470.

Hughes OF, Paik JK. 2010. Ship structural analysis and design. Jersey City: The Society of Naval Architects and Marine Engineers.

IACS. 2006a. Common structural rules for double hull oil tankers. London: International Association of Classification Societies.

IACS. 2006b. Common structural rules for bulk carriers. London: International Association of Classification Societies.

IMO. 2000. SOLAS/2 Recommended longitudinal strength. MSC.108(73). Maritime Safety committee. London: International Maritime Organization.

IMO. 2003. Revised interim guidelines for the approval of alternative methods of design and construction of oil tankers. Marine environmental protection committee of the organization by resolution MEPC 110(49). London: International Maritime Organization.

IMO. 2010. Prevention of air pollution from ships, second IMO GHG study, MEPC 61/INF.10. London: International Maritime Organization.

IMO. 2018. Marine casualties and incidents, global integrated shipping information system (GISIS). London: International Maritime Organization.

IPCC. 2005. Special report of carbon dioxide capture and storage (CCS). Intergovernmental Panel on Climate Change (IPPC). Cambridge: Cambridge University Press.

ISSC. 2009. Ultimate Strength (Committee III.1). The 17th international ship and offshore structures congress (ISSC 2009), 16–21 August, Seoul, Republic of Korea.

ISSC. 2012. Ultimate Strength (Committee III.1). The 18th international ship and offshore structures congress (ISSC 2012), 9–13 September, Rostock, Germany.

ISSC. 2015. Ultimate Strength (Committee III.1). The 19th international ship and offshore structures congress (ISSC 2015), 7–10 September, Cascais, Portugal.

ISSC. 2018. Ultimate Strength (Committee III.1). The 20th international ship and offshore structures congress (ISSC 2018), 9–13 September, Liege, Belgium & Amsterdam, the Netherlands.

Kim DK, Kim SJ, Kim HB, Zhang XM, Li CG, Paik JK. 2015. Ultimate strength performance of bulk carriers with various corrosion additions. Ships Offsh Struct. 10(1):59–78.

Kim JH, Kim SK, Lee CS, Kim MH, Lee JM. 2014. A constitutive equation for predicting the material nonlinear behaviour of AISI. 316L. 321, and 347 stainless steel under low-temperature conditions. Int J Mech Sci. 87:218–225.

Kim DK, Kim HB, Mohd Hairil M, Paik JK. 2013a. Comparison of residual strength-grounding damage index diagrams for tankers produced by the ALPS/HULL ISFEM and design formula method. Int J Naval Archit Ocean Eng. 5(1):47–61.

Kim DK, Kim BJ, Seo JK, Kim HB, Zhang XM, Paik JK. 2014a. Time-dependent residual ultimate longitudinal strength – grounding damage index (R-D) diagram. Ocean Eng. 76:163–171.

Kim DK, Kim HB, Zhang XM, Li CG, Paik JK. 2014b. Ultimate strength performance of tankers associated with industry corrosion addition practices. Int J Naval Archit Ocean Eng. 6(3):507–528.

Kim DK, Park DH, Kim HB, Kim BJ, Seo JK, Paik JK. 2013b. Lateral pressure effects on the progressive hull collapse behaviour of a Suezmax-class tanker under vertical bending moments. Ocean Eng. 63:112–121.

Kim DK, Park DK, Kim HB, Seo JK, Kim BJ, Paik JK, Kim MS. 2012c. The necessity of applying the common addition rule to container ships in terms of ultimate longitudinal strength. Ocean Eng. 49:43–55.

Kim DK, Park DK, Park DH, Kim HB, Kim BJ, Seo JK, Paik JK. 2012b. Effect of corrosion on the ultimate strength of double hull oil tankers - part II: hull girders. Struct Eng Mech. 42(4):531–549.

Kim DK, Park DK, Seo JK, Paik JK, Kim BJ. 2012a. Effect of low temperature on mechanical properties of steel and ultimate hull girder strength of commercial ship. Korean J Met Mater. 50(6):427–432.

Kim DK, Pedersen PT, Paik JK, Kim HB, Zhang XM, Kim MS. 2013c. Safety guidelines of ultimate hull girder strength for grounded container ships. Saf Sci. 59:46–54.

Kim DK, Yu SY, Choi HS. 2013d. Condition assessment of raking damaged bulk carriers under vertical bending moments. Struct Eng Mech. 46(5):629–644.

Mazaheri A, Montewka J, Kujala P. 2016. Towards an evidence-based probabilistic risk model for ship-grounding accidents. Saf Sci. 86:195–210.

Paik JK. 2018. Ultimate limit state analysis and design of plated structures (Second Edition). Chichester: John Wiley & Sons.

Paik JK, Kim DK, Kim MS. 2009. Ultimate strength performance of Suezmax tanker structures: pre-CSR versus CSR designs. Int J Maritime Eng. 151(A2):39–58.

Paik JK, Kim KJ, Lee JH, Jung BG, Kim SJ. 2017. Test database of the mechanical properties of mild, high tensile and stainless steel and aluminium alloy associated with cold temperatures and strain rates. Ships Offsh Struct. 12(1):S230–S256.

Paik JK, Kim BJ, Park DK, Jang BS. 2011. On quasi-static crushing of thin-walled steel structures in cold temperature: experimental and numerical studies. Int J Impact Eng. 38(1):13–28.

Paik JK, Kim DK, Park DH, Kim HB, Kim MS. 2012. A new method for assessing the safety of ships damaged by grounding. Int J Maritime Eng. 154(A1):1–20.

Paik JK, Kim DK, Park DH, Kim HB, Mansour AE, Caldwell JB. 2013. Modified Paik-Mansour formula for ultimate strength calculation of ship hulls. Ships Offsh Struct. 8(3–4):245–260.

Paik JK, Thayamballi AK. 1998. The strength and reliability of bulk carrier structures subject to age and accidental flooding. Trans SocNaval Archit Marine Eng. 106:1–40.

Park DK. 2015. Nonlinear structural response analysis of ships and offshore structures in low temperature [Ph.D. dissertation]. Busan: Department of Naval Architecture and Ocean Engineering, Pusan National University.

Park WS, Chun MS, Han MS, Kim MH, Lee JM. 2011. Comparative study on mechanical behaviour of low temperature application materials for ships and offshore structures: part I - experimental investigation. Mater Sci Eng: A. 528:5790–5803.

Park DK, Kim DK, Park CH, Park DH, Jang BS, Kim BJ, Paik JK. 2015a. On the crashworthiness of steel-plated structures in an Arctic environment: an experimental and numerical study. J Offshore Mech Arct Eng. 137(5):051501.

Park DK, Kim DK, Seo JK, Kim BJ, Ha YC, Paik JK. 2015b. Operability of non-ice class aged ships in the Arctic Ocean – part I:

ultimate limit state approach. Ocean Eng. 102:197–205.

Park DK, Paik JK, Kim BJ, Seo JK, Li CG, Kim DK. 2014. Ultimate strength performance of Northern Sea going non-ice class commercial ships. Struct Eng Mech. 52(3):613–632.

Park WS, Yoo SW, Kim MH, Lee JM. 2010. Strain-rate effects on the mechanical behaviour of the AISI 300 series of austenitic steel under cryogenic environments. Mater Des. 31:3630–3640.

Pedersen PT. 2015. Marine structures: future trends and the role of universities. Engineering. 1(1):131–138.

Ragner CL. 2008. The Northern Sea Route. The barents – a nordic Borderland. T. Hallberg (Ed.), Stockholm, Sweden. p. 114–127).

ScienceDaily. 2018. Arctic cyclone limits the time-scale of precise sea-ice prediction in Northern Sea Route? Rockville (MD): Science News. www.sciencedaily.com/releases/2018/08/180801093700.htm.

Smith CS. 1977. Influence of local compressive failure on ultimate longitudinal strength of ship's hull. The International Symposium on Practical Design in Shipbuilding (PRADS 1977); Tokyo, Japan.

Smith CS, Dow RS. 1981. Residual strength of damaged steel ships and offshore structures. J Constr Steel Res. 1(4):2–15.

SNAK. 2015. Lesson and example of accident in ocean (special report by committee of accident in ocean). Busan: The Society of Naval Architects of Korea (in Korean Language).

Ueda Y, Rashed SMH. 1974. An ultimate transverse strength analysis of ship structures. J Soc Naval Archit Japan. 1974:309–324. (in Japanese).

Ueda Y, Rashed SMH. 1984. The idealized structural unit method and its application to deep girder structures. Comput Struct. 18(2):277–293.

Windén B, Chen M, Okamoto N, Kim DK, McCaig E, Shenoi A, Wilson P. 2014. Investigation of offshore thermal power plant with carbon capture as an alternative to carbon dioxide transport. Ocean Eng. 76:152–162.

Yao T. 2003. Hull girder strength. Marine Struct. 16(1):1–13.

Yoo SW, Lee CS, Park WS, Kim MH, Lee JM. 2011. Temperature and strain rate dependent constitutive model of TRIP steels for low-temperature applications. Comput Mater Sci. 50:2014–2027.

Appendices

Figure A1. Vessel loss scenarios (Paik and Thayamballi 1998). (a) location of grounding damage (p_1) in the direction of the ship's breadth, normalised by ship breadth. (b) height of grounding damage (p_2), normalised by ship depth. (c) breadth of grounding damage (p_3), normalised by ship breadth. (d) Assumed angle of the rock (p_4).

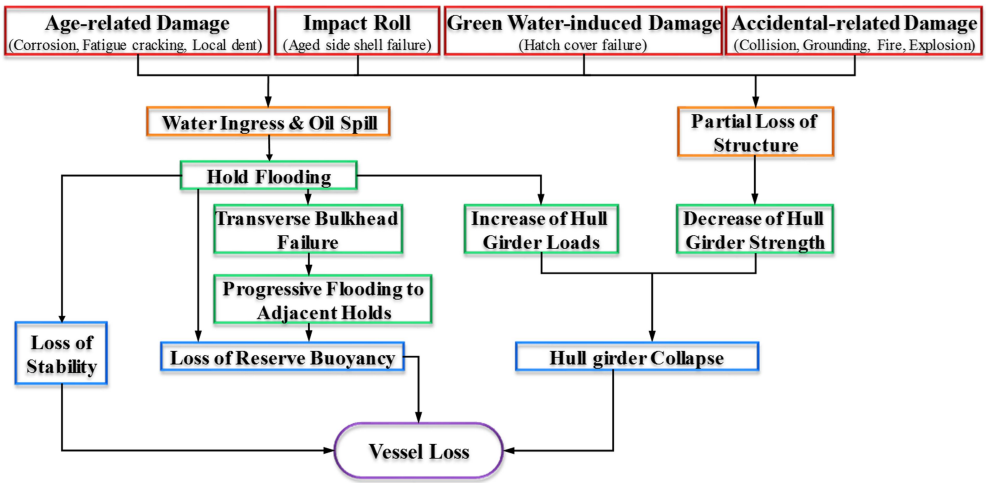

Figure A2. Probability density distributions of damage parameters (IMO 2003; Paik et al. 2012). (a) location of grounding damage (p1) in the direction of the ship's breadth, normalised by ship breadth, (b) height of grounding damage (p2), normalised by ship depth, (c) breadth of grounding damage (p3), normalised by ship breadth and (d) Assumed angle of the rock (p4).

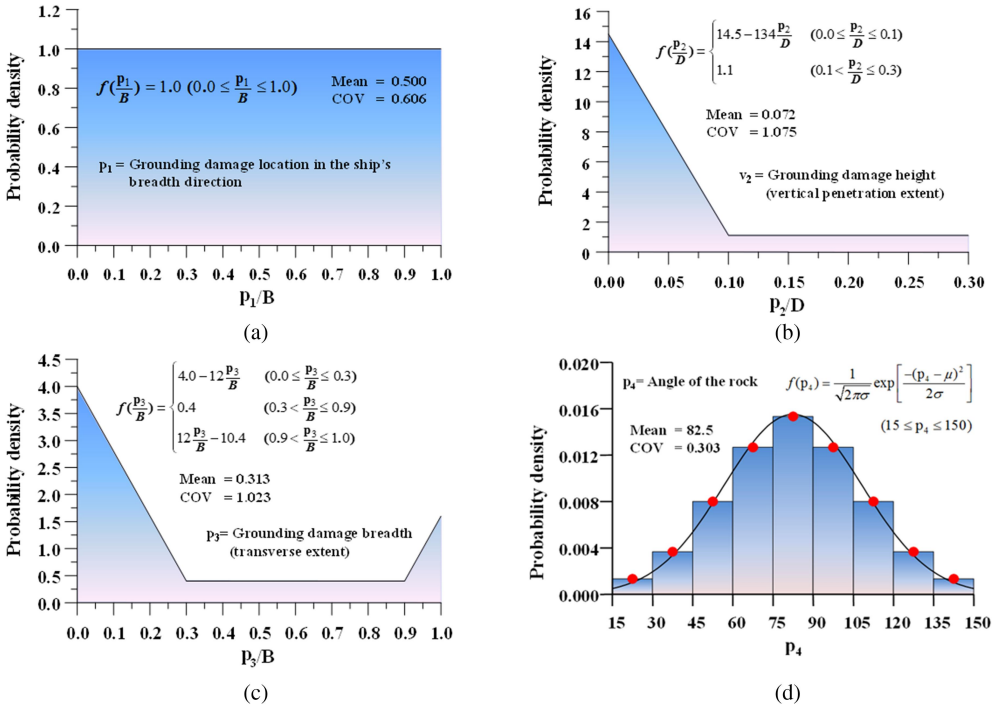

Table A1. Comparison of the distances and potential days saved for Asian transport between SSR and NSR (Emmerson and Lahn 2012).

	Through SSR (Via Suez Canal)			Through NSR			
	Distance (Nm)	Speed (Knots)	Periods (Days)	Distance (Nm)	Speed (Knots)	Periods (Days)	Saving (Days)
Shanghai (China)	12,050	14	37	6500	12.9	21.0	**−16.0**
Busan (South Korea)	12,400	14	38	6050	12.9	19.5	**−18.5**
Yokohama (Japan)	12,730	14	39	5750	12.9	18.5	**−20.5**

Note: SSR = Southern Sea Route, NSR = Northern Sea Route

Table A2. Environmental conditions in NSR (Emmerson and Lahn 2012).

		Environmental conditions in NSR					
Region		Kara Sea		Laptev Sea		East Siberian Sea	
Season		Summer	Winter	Summer	Winter	Summer	Winter
Periods	From	June	October	July	October	Mid-June	October
	To	September	May	September	June	September	May /June
Temperature (°C)	Typical	7°C	−26°C	8°C	−30°C	15°C	−21°C
	Extreme	20°C	−48°C	26°C	−50°C	30°C	−48°C
Thickness of ice (m)		–	1.8–2.5m	–	1.6–2.5m	–	1.2–2.0m
Duration of fog (days)		–	100 days	–	75 days	–	80 days